

Journal of
Applied Remote Sensing

**Mapping herbage biomass and
nitrogen status in an Italian
ryegrass (*Lolium multiflorum*
L.) field using a digital
video camera with
balloon system**

Kensuke Kawamura
Yuji Sakuno
Yoshikazu Tanaka
Hyo-Jin Lee
Jihyun Lim
Yuzo Kurokawa
Nariyasu Watanabe

Mapping herbage biomass and nitrogen status in an Italian ryegrass (*Lolium multiflorum* L.) field using a digital video camera with balloon system

Kensuke Kawamura,^a Yuji Sakuno,^b Yoshikazu Tanaka,^b
Hyo-Jin Lee,^a Jihyun Lim,^a Yuzo Kurokawa,^c and
Nariyasu Watanabe^d

^aHiroshima University, Graduate School for International Development and Cooperation,
1-5-1 Kagamiyama, Higashi-Hiroshima, Hiroshima 739-8529, Japan

kamuken@hiroshima-u.ac.jp; tallwind25@gmail.com; limjihyun7@gmail.com

^bHiroshima University, Graduate School of Engineering, 1-4-1 Kagamiyama,
Higashi-Hiroshima, Hiroshima 739-8527, Japan

sakuno@hiroshima-u.ac.jp; yoshi@naoe.hiroshima-u.ac.jp

^cHiroshima University, Graduate School of Biosphere Science, Kagamiyama 2-2965,
Higashi-Hiroshima, Hiroshima 739-0046, Japan

yuzokuro@hiroshima-u.ac.jp

^dNARO Hokkaido Agricultural Research Center, 1 Hitsujigaoka, Toyohira-ku, Sapporo,
Hokkaido 062-8555, Japan

nariyasu@affrc.go.jp

Abstract. Improving current precision nutrient management requires practical tools to aid the collection of site specific data. Recent technological developments in commercial digital video cameras and the miniaturization of systems on board low-altitude platforms offer cost effective, real time applications for efficient nutrient management. We tested the potential use of commercial digital video camera imagery acquired by a balloon system for mapping herbage biomass (BM), nitrogen (N) concentration, and herbage mass of N (N_{mass}) in an Italian ryegrass (*Lolium multiflorum* L.) meadow. The field measurements were made at the Setouchi Field Science Center, Hiroshima University, Japan on June 5 and 6, 2009. The field consists of two 1.0 ha Italian ryegrass meadows, which are located in an east-facing slope area (230 to 240 m above sea level). Plant samples were obtained at 20 sites in the field. A captive balloon was used for obtaining digital video data from a height of approximately 50 m (approximately 15 cm spatial resolution). We tested several statistical methods, including simple and multivariate regressions, using forage parameters (BM, N, and N_{mass}) and three visible color bands or color indices based on ratio vegetation index and normalized difference vegetation index. Of the various investigations, a multiple linear regression (MLR) model showed the best cross validated coefficients of determination (R^2) and minimum root-mean-squared error (RMSECV) values between observed and predicted herbage BM ($R^2 = 0.56$, RMSECV = 51.54), N_{mass} ($R^2 = 0.65$, RMSECV = 0.93), and N concentration ($R^2 = 0.33$, RMSECV = 0.24). Applying these MLR models on mosaic images, the spatial distributions of the herbage BM and N status within the Italian ryegrass field were successfully displayed at a high resolution. Such fine-scale maps showed higher values of BM and N status at the bottom area of the slope, with lower values at the top of the slope. © 2011 Society of Photo-Optical Instrumentation Engineers (SPIE). [DOI: [10.1117/1.3659893](https://doi.org/10.1117/1.3659893)]

Keywords: balloon; digital video camera; herbage biomass; nitrogen status; spatial distribution; precision agriculture.

Paper 11029RR received Feb. 20, 2011; revised manuscript received Oct. 19, 2011; accepted for publication Oct. 21, 2011; published online Nov. 14, 2011.

1 Introduction

Recently developed site-specific agricultural management systems, also known as precision agriculture, provide a method that involves cost reduction, optimization of crop yield, and environmental protection.¹ Precision agriculture consists of applying fertilizer only where necessary and with only the exact amount of product needed. This requires that reliable monitoring and proper analysis methodologies are developed to allow the efficient integration of the spatial distributions of crop, soil, and environmental factors. However, there are two major barriers to the wider use of spatial models and tools: the cost and difficulty of collecting spatially discrete data sets.² For example, current precision nutrient management requires the collection of a large amount of data within the field rather than at block or field level as uniform pieces of land. This is neither practical nor cost effective using traditional ground-based plant sampling methods. Similarly, using traditional approaches for establishing and managing the nutrient status of crops and soils in and around waterways as part of an overall nutrient management package is also impractical due to a need for extensive data sets to characterize the nutrient profiles across the landscape. Thus, techniques need to be developed that can measure the nutrient status quickly and cost-effectively and can provide continuous data across the landscape.

Remotely sensed imagery is one of the most effective tools for displaying the spatial variation in forage condition within fields. Numerous studies have been conducted on grassland diagnosis using airborne or satellite remote sensing. However, useful satellite imagery is not always available, partly because cloud cover often hampers data acquisition and the time needed for the satellite to collect repeat images in the same location is relatively long (e.g., every 16 days for Landsat).^{3,4} Another limitation of imagery acquired from satellite platforms is the low spatial resolution (e.g., 30 m for Landsat). Airborne imaging sensors offer much greater flexibility than satellite platforms by being able to operate under clouds and having a much finer spatial resolution.⁵ However, the practical use of this type of imagery is still expensive when repeated data acquisition is needed. To overcome these problems, there have been several attempts to collect imagery using low-altitude aerial platforms, such as blimps,⁶ remote-control helicopters,^{7,8} and cable-supported helium balloon systems.^{9,10} Low-altitude aerial platform systems can provide fine-scale imagery (<1 m) through the crop growing season in a cost effective manner.

Although film cameras and video systems have been used on low-altitude aerial platforms since the 1980s,¹¹ recent technological developments in digital video cameras and the miniaturization of systems offer new, innovative applications for efficient nutrient management. Digital video techniques have a number of significant advantages over remote sensing applications for agricultural land.^{11,12} The most significant advantage is the immediate availability of imagery, which is important in highly time-sensitive applications, such as monitoring agricultural crops and disaster assessment. Moreover, the digital format of video data allows for easy image processing using a number of image processing software packages (e.g., ERDAS, ENVI). Furthermore, the market price of a digital video camera is becoming lower every year, and with the new hard disk storage system employed by digital video cameras, there is no cost for film.

Italian ryegrass (*Lolium multiflorum* L.) is one of the most important and widely cultivated annual, cool-season forage grass species in Japan. It is available to farmers for hay and for making silage for animals in the winter. Prior studies have found several factors influencing the biomass (BM) production and nutrient status of Italian ryegrass meadows, such as soil,^{13,14} nutrient supply,^{15,16} and air temperature.¹⁷ However, most of these findings were based on block-level analysis, and these factors may vary within a field due to micrometeorology and geography. Moreover, most Italian ryegrass in Japan is cultivated on a small land area and located on mountainous or hilly land, making it difficult to manage precisely. Therefore, development precision management systems requires a quick, cost effective tool for making site-specific detection of spatial variance of herbage BM and nitrogen (N) status as a very fine resolution map.

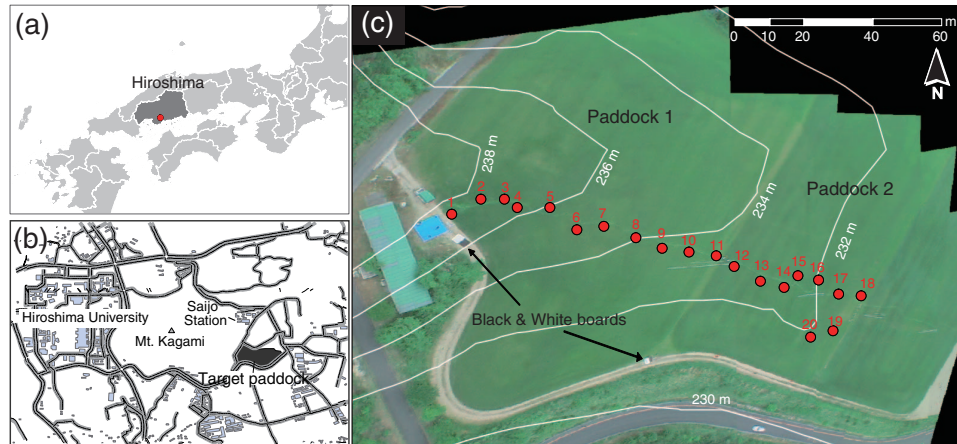


Fig. 1 The location of the experimental paddock [(a) and (b)] and the mosaic image acquired by the digital video camera on a balloon system used in this study (c), which indicate the locations of the 20 plant sampling points and black-and-white boards on the study site.

In the present study, for the purpose of developing a simple and cost effective low-altitude aerial platform system using a commercial digital video camera on a balloon system for making a fine resolution map of herbage BM and N status, we collected the images in an Italian ryegrass field, and then attempted an estimation of the herbage BM, N concentration, and standing mass of N (N_{mass}) using statistical analyses.

2 Materials and Methods

2.1 Study Area

The study was conducted in two 1.0-ha fields of Italian ryegrass meadows at the Setouchi Field Science Center, Saijo Station ($34^{\circ} 23' \text{N}$, $132^{\circ} 43' \text{E}$), Graduate School of Biosphere Science, Hiroshima University (Fig. 1). In the farm, Italian ryegrass is usually used as a main winter forage crop, with seeding in the autumn season and harvest twice in mid-April and early June. At the time of field measurements on June 5 and 6, 2009, the Italian ryegrass secondary growth meadows were at heading stage. The fields were located in an east-facing slope area. The elevation ranged from 230 to 240 m above sea level, and the mean slope angle was approximately 5 deg. The climate of the study site was a temperate zone with warm, humid summers and cool, dry winters. The annual mean temperature was 14.6°C , and the annual precipitation was 621.9 mm in 2008.

Fertilizer was applied to the fields on November 12, 2008 in field 1 (N:phosphorus [P_2O_5]:potassium [K_2O] = 127:135:41 kg ha^{-1}) and on November 13, 2008 in field 2 (N: P_2O_5 : K_2O = 25:25:25 kg ha^{-1}). Additional fertilizer was applied on March 9, 2009 in field 1 (N: P_2O_5 : K_2O = 29:0:0 kg ha^{-1}) and on March 10, 2009 (N: P_2O_5 : K_2O = 29:0:0 kg ha^{-1}) and May 13, 2009 (N: P_2O_5 : K_2O = 46:0:0 kg ha^{-1}) in field 2.

2.2 Digital Video Data and Balloon System

A captive balloon, developed by Sakuno et al.⁹ for monitoring the seagrass bed area at sea, was used for obtaining digital video data from a height of approximately 50 m in the nadir position (Fig. 2), giving approximately 15 cm spatial resolution on the ground. The balloon, filled with approximately 21 m^3 of helium gas with length (between nose and tail of balloon) of 5 m and maximum diameter of 2.4 m, was able to lift a 5 kg payload. The shape was designed to operate



Fig. 2 Picture of the digital video camera and balloon system used in this study.

stably up to 4 m s^{-1} wind speed. Therefore, the wind speed, during which the balloon operation ranged from 0.1 to 0.5 m s^{-1} (Hiroshima University Meteorological Data Acquisition System; <http://home.hiroshima-u.ac.jp/hirodas/>), did not affect the balloon operation. The height and direction of balloon operation were controlled by pulling the rope.

A commercial digital video camera (HDC-HS9-S, Panasonic Co. Ltd., Tokyo, Japan) was mounted on the balloon's gondola. The digital video data (1920×1080 pixels) was recorded in the 64 GB hard disk. The total weight of the system was 1.0 kg, with a run time of 90 min using the default video camera battery.

The construction cost of the balloon system including the video camera was about \$5000 (U.S.), and each operation needs a running cost about \$800 (U.S.) for helium gas. Balloon operation time, including setup and flying at the target area, was approximately 30 min, and the processing took approximately 180 min to be done from the balloon setup to post-processing of mosaic image. The time taken for the post-processing is expected to be reduced by automating the process in the future.

2.3 Image Preprocessing

Five captured images from the digital video data were used in this study to cover the entire area of the target field. Image processing was performed using ENVI/IDL software ver. 4.2 (ITT Co. Ltd., Boulder, Colorado). First, the 8-bit digital number (DN) values for the red (DN_{red}), green (DN_{green}), and blue (DN_{blue}) bands were calibrated for light intensity using two black-and-white boards ($90 \text{ cm} \times 180 \text{ cm}$) placed out of the field (see Fig. 1). Then, each image was georeferenced using ground control points that were collected with the differentially corrected global positioning system (DGPS) receiver Hemisphere A100 GPS (Hemisphere Co. Ltd., Calgary, Canada), giving an accuracy of less than 1 m. Each georeferenced image was remapped to a UTM projection with 15 cm pixels as a GeoTIFF file. Finally, a mosaic image in the target field was obtained using the automated color balancing function in ENVI software. Although earlier studies indicated the importance of canopy segmentation on image processing in vision-based remote sensing,^{18,19} the present study did not perform a segmentation procedure because the ground surface at the time of field experiment was almost 100% vegetation covered in the target area of the Italian ryegrass meadow field.

2.4 Field Data Collection and Chemical Analysis

Forage sampling was conducted in 20 plots within the field on June 5 to 6, 2009 (Fig. 1). All vegetation was clipped to ground level using a $1 \text{ m} \times 1 \text{ m}$ quadrat. The forage samples were

dried in a forced-air oven at 65°C for 72 h to determine the dry matter (DM) of the BM (gDM m⁻²). Chemical analyses were performed at the Federation of Tokachi Agricultural Cooperative Association Agricultural Product Chemical Research Laboratory. The N concentration was determined by laboratory near-infrared spectroscopy. Then, the nutritive mass of N (N_{mass}, gDM m⁻²) was obtained by multiplying BM by N concentration.

2.5 Statistical Analyses

The statistical analyses included descriptive, correlation, simple, and multiple linear regression (MLR) analyses using MATLAB software version 7.7 (Mathworks Inc., Sherborn, Massachusetts). Two visible color indices, a ratio color index (RCI), and a normalized difference color index (NDCI), were calculated based on a ratio vegetation index²⁰ and a normalized difference vegetation index²¹ for all available band combinations using the red, green, and blue bands, as follows:

$$RCI_{[\text{band1}, \text{band2}]} = DN_{\text{band1}} / DN_{\text{band2}}, \quad (1)$$

$$NDCI_{[\text{band1}, \text{band2}]} = (DN_{\text{band1}} - DN_{\text{band2}}) / (DN_{\text{band1}} + DN_{\text{band2}}), \quad (2)$$

where DN_{band1} and DN_{band2} are DN values for all available combinations in the red, green, and blue bands, respectively. Simple linear regression analyses used each band and the two vegetation indices. MLR analysis used all bands to estimate pasture parameters. For the accuracy assessment of the calibration models, this study employed leave-one-out cross-validation due to a small number of data sets and a single image. The predictive ability was evaluated by the cross-validated coefficient of determination (R^2) and the root-mean-squared error (RMSECV) values.

3 Results and Discussion

3.1 Relationship Between Digital Video Color Bands and Pasture Parameters

Table 1 shows the results of the descriptive analysis for BM, N, and N_{mass} with correlation coefficients (r) among the parameters. The mean values of BM, N, and N_{mass} were 306 gDM m⁻², 1.6% DM, and 4.9 gDM m⁻², respectively. A wider range of N_{mass} [coefficient of variation (CV) = 33.0] than BM (CV = 25.9) and N (CV = 19.2) exhibited better predictive accuracy for N_{mass} because regression analysis needs a wide range of sample data to develop a calibration model. Among the parameters, a significantly positive correlation was found between N_{mass} and BM ($r = 0.83$, $P < 0.001$), and N ($r = 0.75$, $P < 0.001$).

Figure 3 shows the relationships between each band and BM, N, and N_{mass}. The G band was closely correlated with BM ($r = 0.68$, $P < 0.001$) and N_{mass} ($r = 0.71$, $P < 0.001$). A similar, positive correlation was found between the green band and N concentration ($r = 0.49$, $P < 0.05$). There was a close, negative correlation between the red band and BM ($r = -0.70$, $P < 0.001$) and N_{mass} ($r = -0.77$, $P < 0.001$). Also, negative correlations were found between the red band and N concentration ($r = -0.55$, $P < 0.05$) and between the blue band and BM and N_{mass} ($r = -0.48$, $P < 0.05$). Similar tendencies in the visible channel (blue, green, and red bands) were reported by Inoue and Morinaga²² when they analyzed the digital image data at spectral bands of blue, green, red, and near-infrared (NIR) wavelength regions in a soybean field (*Glycine max* Merr.). They also indicated that the best correlation was found at the NIR band with biomass ($r = 0.982$).

Table 1 Descriptive statistics of the aboveground BM, N concentration, and standing mass of N (N_{mass}) in the target paddock, with correlation coefficients among the parameters.

Pasture parameters	Mean	Min	Max	SD ^a	CV ^b	Correlations among parameters		
						BM	N	N_{mass}
Aboveground biomass (BM, gDM m ⁻²)	306.7	158.8	449.6	79.5	25.9	1		
Nitrogen concentration (N, % DM)	1.6	1.0	2.2	0.3	19.2	0.27	1	
Standing mass of N (N_{mass} , gDM m ⁻²)	4.9	1.7	7.7	1.6	33.0	0.83 ^c	0.75 ^c	1

^aStandard deviation (SD).

^bCV for $n = 20$ data.

^cSignificant at the probability level of 0.1%.

3.2 Estimation of Herbage BM and N Status

This study applied several statistical methods to predict herbage BM, N concentration, and N_{mass} in an Italian ryegrass field. Figure 4 shows the RMSECV between laboratory-measured pasture parameters and the predicted values from regression analyses. In the single band using the simple regression analyses, the lowest RMSECV was obtained in the red band for all parameters.

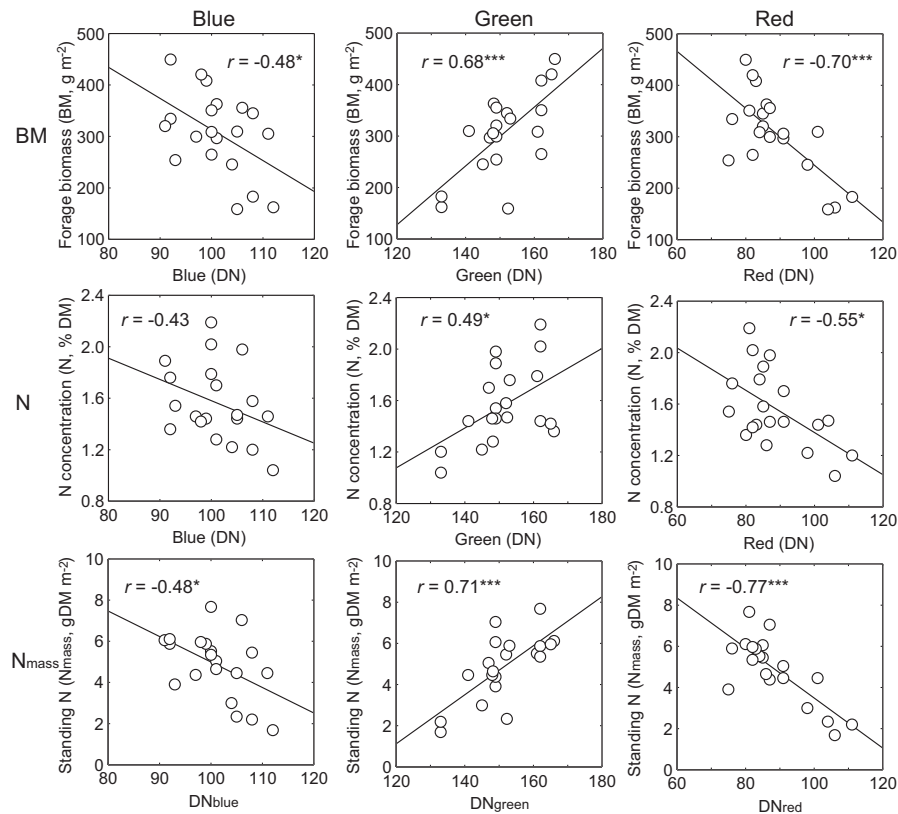


Fig. 3 The relationships between three visible color bands and herbage BM, N concentration, and standing herbage mass of N (N_{mass}).

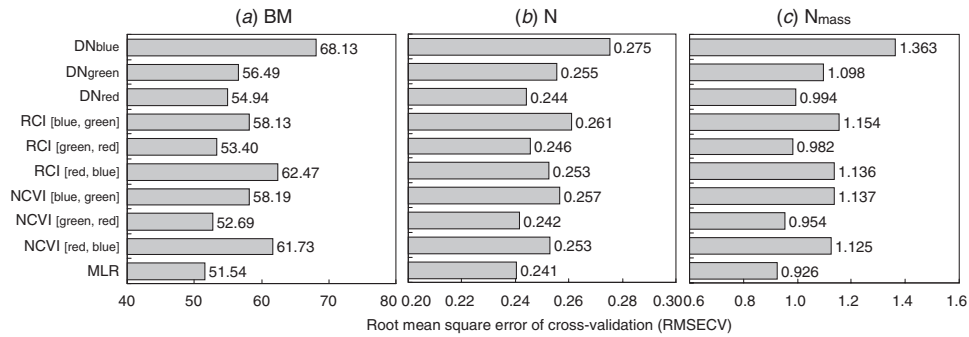


Fig. 4 RMSECV between laboratory-measured and predicted BM, N concentration, and N_{mass} from regression analyses.

In the analysis using all available two band combinations based on NDCI and RCI forms, the best indices for estimating BM, N, and N_{mass} were the green and red NDCI. The spectral reflectance of plants in the blue, green, and red regions is primarily determined by pigments, often chlorophyll concentration, and has therefore been widely used to quantify the physiological properties of vegetation, such as biomass and leaf area index. The bands in the visible region are related to absorption by chlorophyll a (centered at 430- and 660-nm wavelengths) and chlorophyll b (centered at 460 and 640 nm),^{23,24} which correlate strongly with nutritive value and chlorophyll production and activity.

Overall, MLR models showed the minimum RMSECV values in all pasture parameters, and the validation plots (Fig. 5) showed a strong linear relationship between measured and predicted values of BM ($R^2 = 0.56$, RMSECV = 51.54) and N_{mass} ($R^2 = 0.65$, RMSECV = 9.26), although relatively low accuracy was determined for N ($R^2 = 0.33$, RMSECV = 2.41). This is in agreement with previous studies that have demonstrated that better predictive accuracy is obtained in multivariable regression than in vegetation indices (VIs).^{25–27} It is presumed that the predictive accuracy of a commercial video camera based on low-altitude remote sensing could not be better than that of multispectral visible-NIR imagery from a balloon system²² and a ground-based multispectral sensor.²⁸ These previous findings may indicate that the predictive accuracy of future studies should improve by combining NIR spectral band images with our system. Nevertheless, the models developed in this study, with the best R^2 reaching 0.56 for BM and 0.65 for N_{mass} , can cost-effectively provide quantitative information on BM and nutrient status at the geospatial level and on a near real-time basis over a wide area. Thus, these models have great potential for efficient, productive, and practical pasture management.

3.3 Spatial Distribution Maps of Herbage BM and N Status

Applying the MLR models on the digital video images, spatial distribution maps of BM, N, and N_{mass} were obtained with the digital elevation map (DEM), as shown in Fig. 6. The spatial variations of BM (143.2 to 552.4 gDM m⁻²), N (0.8 to 2.4% DM), and N_{mass} (1.5 to 9.0 gDM

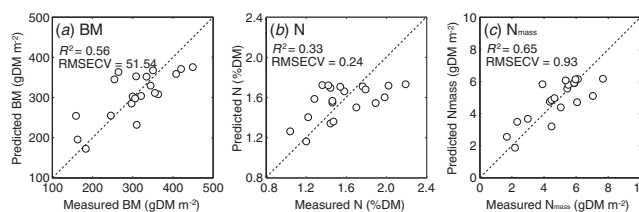


Fig. 5 Measured and predicted values of BM, N concentration, and N_{mass} using MLR models.

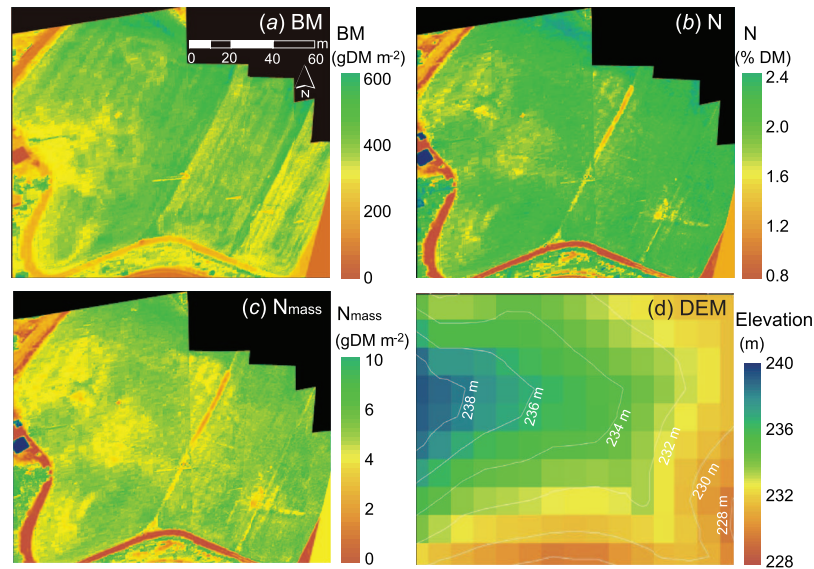


Fig. 6 Predicted spatial distribution maps of (a) BM, (b) N, (c) N_{mass} , and (d) DEM (10-m grid cell) with a 2-m contour line in the target paddock.

m^{-2}) showed similar tendencies in that the values increased from top to bottom, following a geographical gradient. In Japan, most Italian ryegrass meadows are established on hillsides or in mountainous regions with sloping ground in a small-scale field. The fine-scale maps obtained with our results suggests that the fertilizer flowed toward the bottom of the slope. Such fine-scale and near real-time information could support a farmer in decision making for an appropriate cutting date to improve hay quality. However, we should note that the data collection in this study was just before harvest because of the weather condition. Early detection of herbage BM and N status is important to make follow-up treatments effective.

It is obvious that insufficient spatial distribution due to sparse spatial resolution and similarity of spectral properties of weeds and crops impedes the determination of spatial heterogeneity of plant production and the discrimination of individual plants. Only sensor platforms at lower altitudes, such as drones and balloons, could minimize pixel size to even a few millimeters and so overcome the spatial resolution problems.²⁹ However, geometry and illumination problems would still remain. The geometric correction in this study, which used only DGPS ground information, needs further investigation on accurate measuring of the position and posture of the balloon. Nevertheless, our study indicated that a digital video camera mounted on a balloon system successfully displayed the spatial distribution of plant status within an Italian ryegrass field. Earlier detection of herbage BM and N status as fine-scale maps would be useful information for farmers in the optimization of grassland management, which could be realized by controlling spatial heterogeneity using patch-spraying fertilizer application technology.

4 Conclusions

In this study, we examined the potential use of a commercial digital video camera on a balloon platform as a cost-effective tool for mapping herbage BM and N status in an Italian ryegrass field. Our results indicated that the herbage BM and N status can be estimated and mapped from the digital video camera's color information with MLR analysis. The spatial distribution maps showed higher values of BM and N status at the bottom area of the slope, with lower values at the top of the slope. The advantages of this system are its ease of handling and the cost-effective provision of high-resolution images. These fine-scale maps could provide some

useful insights for the optimization of grassland management; we expect that a farmer could use them to support decision making in appropriate timing and strategy for cutting, and to develop a precision nutrient management plan with earlier observation. Further investigations in different seasons with improvements in geometric correction and digital video systems are left to future studies.

Acknowledgments

We are grateful to all the staff of the Setouchi Field Science Center, Saijo Station, Hiroshima University, for their assistance in field experiments. This work was supported by funding from the Hiroshima University Foundation.

References

1. J. Bouma, "Precision agriculture: introduction to the spatial and temporal variability of environmental quality," in *Ciba Foundation Symposium*, J. V. Lake, G. R. Bock, and J. A. Goode, Eds., pp. 5–17, John Wiley and Sons, Wageningen, The Netherlands (1997).
2. K. Betteridge, E. Schnug, and S. Haneklaus, "Will site specific nutrient management live up to expectation?," *Landbauforschung, vTI Agriculture and Forestry Research* **58**, 283–294 (2008).
3. T. Akiyama and K. Kawamura, "Study of cloud cover ratio of Landsat-5 for the application on agriculture and forestry," *J. Jpn. Soc. Photogrammetry and Remote Sensing* **42**, 29–34 (2003).
4. R. D. Graetz, "Satellite remote sensing of Australian rangelands," *Remote Sens. Environ.* **23**, 313–331 (1987).
5. D. W. Lamb and R. B. Brown, "PA—precision agriculture: Remote-sensing and mapping of weeds in crops," *J. Agric. Eng. Res.* **78**, 117–125 (2001).
6. Y. Inoue, S. Morinaga, and A. Tomita, "A blimp-based remote sensing system for low-altitude monitoring of plant variables: A preliminary experiment for agricultural and ecological applications," *Int. J. Remote Sens.* **21**, 379–385 (2000).
7. R. Sugiura, N. Noguchi, and K. Ishii, "Remote-sensing technology for vegetation monitoring using an unmanned helicopter," *Biosystems Eng.* **90**, 369–379 (2005).
8. F. Rovira-Más, Q. Zhang, and J. F. Reid, "Creation of three-dimensional crop maps based on aerial stereoimages," *Biosystems Eng.* **90**, 251–259 (2005).
9. Y. Sakuno, S. Luy, H. Kunii, Y. Tanaka, E. Kunisada, and Y. Wakamatsu, "Estimating spatial distribution of seagrass bed area in the Nakaumi from balloon on-boarded video camera," *J. Hydrosoci. Hydraulic Eng.* **53**, 1357–1362 (2009). (in Japanese with English abstract).
10. T. Jensen, A. Apan, F. Young, and L. Zeller, "Detecting the attributes of a wheat crop using digital imagery acquired from a low-altitude platform," *Comput. Electron. Agric.* **59**, 66–77 (2007).
11. D. E. Meisner, "Fundamentals of airborne video remote sensing," *Remote Sens. Environ.* **19**, 63–79 (1986).
12. T. Akiyama, "Grasslands and remote sensing 3: Data acquisition from low-altitude platforms and image analysis for grassland management," *Jpn. J. Grassl Sci.* **39**, 505–514 (1994). (in Japanese).
13. K. Ikeda, Y. Nonoyama, and M. Ichiki, "Effect of exchangeable base content in the soil on the yield and base balance of Italian ryegrass," *Jpn. J. Soil Sci. Plant Nutr.* **70**, 51–58 (1999). (in Japanese with English abstract).
14. K. F. Nielsen and R. K. Cunningham, "The effects of soil temperature and form and level of nitrogen on growth and chemical composition of Italian ryegrass," *Soil Sci. Soc. Am. J.* **28**, 213–218 (1964).

15. D. Wilman, "The effect of nitrogenous fertilizer on the rate of growth of Italian ryegrass," *Grass Forage Sci.* **20**, 248–254 (1965).
16. D. Wilman, "Nitrogen and Italian ryegrass. 1. Growth up to 14 weeks: Dry-matter yield and digestibility," *Grass Forage Sci.* **30**, 141–147 (1975).
17. J. D. H. Keatinge, M. K. Garrett, and R. H. Stewart, "Response of perennial and Italian ryegrass cultivars to temperature and soil water potential," *J. Agric. Sci.* **94**, 171–176 (1980).
18. A. Laliberte and A. Rango, "Image processing and classification procedures for analysis of sub-decimeter imagery acquired with an unmanned aircraft over arid rangelands," *GISci. Remote Sens.* **48**(1), 4–23 (2011).
19. R. Breckenridge and M. Dakins, "Evaluation of bare ground on rangelands using unmanned aerial vehicles: A case study," *GISci. Remote Sens.* **48**(1), 74–85 (2011).
20. C. F. Jordan, "Derivation of leaf-area index from quality of light on the forest floor," *Ecology* **50**, 663–666 (1969).
21. J. W. Rouse, R. H. Haas, J. A. Schell, D. W. Deering, and J. C. Harlan, "Monitoring the vernal advancement of retrogradation of natural vegetation," Ed. NASA/GSFC, Maryland, pp. 1–371 (1974).
22. Y. Inoue and S. Morinaga, "Estimating spatial distribution of plant growth in a soybean field based on remotely-sensed spectral imagery measured with a balloon system," *Jpn. J. Crop Sci.* **64**, 156–158 (1995).
23. P. J. Curran, "Remote sensing of foliar chemistry," *Remote Sens. Environ.* **30**, 271–278 (1989).
24. P. J. Curran, J. L. Dungan, and D. L. Peterson, "Estimating the foliar biochemical concentration of leaves with reflectance spectrometry: Testing the Kokaly and Clark methodologies," *Remote Sens. Environ.* **76**, 349–359 (2001).
25. R. Darvishzadeh, A. Skidmore, M. Schlerf, C. Atzberger, F. Corsi, and M. Cho, "LAI and chlorophyll estimation for a heterogeneous grassland using hyperspectral measurements," *ISPRS J. Photogramm.* **63**, 409–426 (2008).
26. H. T. Nguyen and B.-W. Lee, "Assessment of rice leaf growth and nitrogen status by hyperspectral canopy reflectance and partial least square regression," *Eur. J. Agron.* **24**, 349–356 (2006).
27. M. Kanemoto, S. Tanaka, K. Kawamura, H. Matsufuru, K. Yoshida, and T. Akiyama, "Wavelength selection for estimating biomass, LAI, and leaf nitrogen concentration in winter wheat of Gifu prefecture using *in situ* hyperspectral data," *Jpn. J. Agric. Syst. Soc.* **24**, 43–56 (2008). (in English with Japanese abstract).
28. S. Itano, T. Akiyama, N. Watanabe, T. Okubo, and Y. Hashimoto, "The determination of growth condition in Italian ryegrass (*Lolium multiflorum* Lam.) meadows with a hand-held spectrometer," *Grassland Sci.* **47**, 237–244 (2001).
29. S. Gebhardt and W. Kühbauch, "A new algorithm for automatic *Rumex obtusifolius* detection in digital images using colour and texture features and the influence of image resolution," *Precision Agriculture* **8**, 1–13 (2007).

Biographies and photographs of the authors not available.